Genetic control of cell morphogenesis during *Drosophila melanogaster* cardiac tube formation

Caroline Medioni,[1] Martine Astier,[1] Monika Zmojdzian,[2] Krzysztof Jagla,[2] and Michel Sémériva[1]

[1]Institut de Biologie du Développement de Marseille-Luminy, Centre National de la Recherche Scientifique UMR 6216, Université de la Méditerranée, 13288 Marseille, Cedex 9, France
[2]Unité Mixte de Recherche, Institut National de la Santé et de la Recherche Médicale et Centre National de la Recherche Scientifique 6247-Genetique, Reproduction et Developpement, Université de Clermont-Ferrand, 63000 Clermont-Ferrand, France

Tubulogenesis is an essential component of organ development, yet the underlying cellular mechanisms are poorly understood. We analyze here the formation of the *Drosophila melanogaster* cardiac lumen that arises from the migration and subsequent coalescence of bilateral rows of cardioblasts. Our study of cell behavior using three-dimensional and time-lapse imaging and the distribution of cell polarity markers reveals a new mechanism of tubulogenesis in which repulsion of prepatterned luminal domains with basal membrane properties and cell shape remodeling constitute the main driving forces. Furthermore, we identify a genetic pathway in which *roundabout*, *slit*, *held out wings*, and *dystroglycan* control cardiac lumen formation by establishing nonadherent luminal membranes and regulating cell shape changes. From these data we propose a model for *D. melanogaster* cardiac lumen formation, which differs, both at a cellular and molecular level, from current models of epithelial tubulogenesis. We suggest that this new example of tube formation may be helpful in studying vertebrate heart tube formation and primary vasculogenesis.

Introduction

Biological tubes are fundamental structural and functional units of tissue architecture. The cardiovascular system and most internal organs, such as kidney, liver, heart, and lungs, are composed of simple tubes or of a network of tubes that transport fluids or gases. During tubulogenesis, cell polarity, shape, and size must be precisely controlled and cellular adherens junctions need to be continuously remodeled. Unraveling the mechanisms underlying such membrane dynamics is crucial to understand various pathologies including metastasis and tumor progression.

Our knowledge of tubulogenesis has increased considerably during the last decade. Several studies proposed that the main steps may be shared by diverse pathways of tubulogenesis (Lubarsky and Krasnow, 2003; Kerman et al., 2006).

However, it is not clear whether these general features are relevant to the formation of all tubes. In particular, morphogenesis of the dorsal aorta, the posterior cardinal vein, and the primitive vertebrate heart tube appear to involve different mechanisms. In fish, major axial vessels are formed by the migration of angioblasts originating from the lateral plate mesoderm, which coalesce in the midline (Weinstein, 1999; Jin et al., 2005). Recently, Jin et al. (2005) reported a cellular and molecular analysis of vascular tube and lumen formation in zebrafish, showing the coalescence of angioblasts at the midline to form aggregates or solid cords. Within these aggregates, endothelial cell–cell contacts are established, and subsequently a tube with a lumen becomes apparent. The membrane walls of the lumen display some characteristics of basal membranes, as they express, for example, integrins and extracellular matrix components (Davis and Senger, 2005). However, the mechanisms of cell migration, polarity, and shape remodeling underlying lumen formation remain largely unknown.

Drosophila melanogaster cardiac tube morphogenesis shares remarkable similarities with the formation of primary axial vessels in vertebrates. Indeed, it has been recently proposed (Hartenstein and Mandal, 2006) that the *D. melanogaster* cardiovascular system is phylogenetically related to the vertebrate vascular system. The cardiovascular system in flies is formed by a simple linear tube, which constitutes the unique vessel of an open

Correspondence to Caroline Medioni: medioni@ibdml.univ-mrs.fr

Abbreviations used in this paper: Arm, Armadillo; CB, cardioblast; DE-Cad, DE-cadherin; Dg, Dystroglycan; Dlg, Discs large; How, Held out wings; Lgl, Lethal giant larvae; Robo, Roundabout; Shg, Shotgun; Trol, Terribly reduced optic lobes; UAS, upstream activating sequence.

The online version of this article contains supplemental material.

The Rockefeller University Press $30.00
J. Cell Biol. Vol. 182 No. 2 249–261
www.jcb.org/cgi/doi/10.1083/jcb.200801100

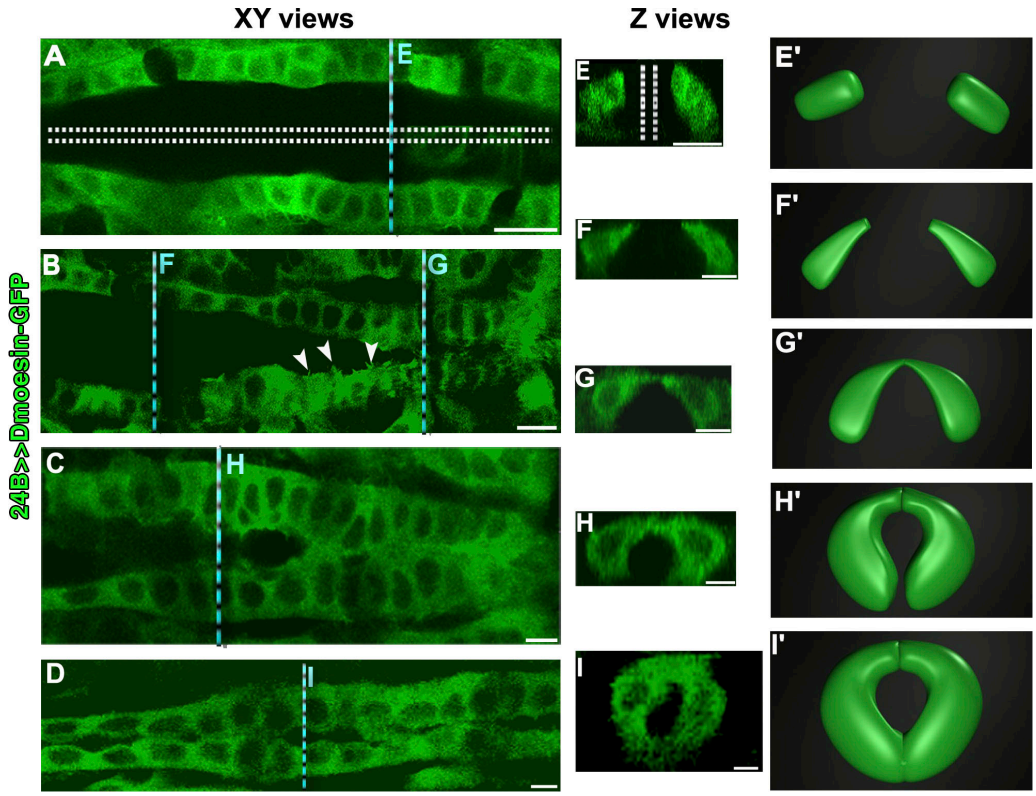

Figure 1. **Cardiac lumen formation.** Sequence of events extracted from Video 1 (available at http://www.jcb.org/cgi/content/full/jcb.200801100/DC1). Dorsal XY views (A–D) and transverse Z views (E–I) of CBs at different time points during cardiac tube formation (from stages 13–14 to 16–17 of embryogenesis). (E′–I′) Schematic 3D views of CBs in E–I. Blue dashed lines show the Z section positions. UAS Dmoesin-GFP; 24B-Gal4 flies were used to follow CB shape remodeling. (A, E, and E′) At the onset of migration, CBs have a square shape. (B, F, and F′) Subsequently, during their migration they constrict, adopt a triangular shape, and form a dorsal leading edge. (B, G, and G′) Soon after, CBs adopt a pearlike shape and the cells join at the dorsal leading edge. (C, H, and H′) After joining dorsally, CBs take a crescentlike shape that brings their ventral sides into proximity. (D, I, and I′) Finally, CBs join ventrally to close the tube and form the lumen. At the end of embryogenesis, CBs and the lumen grow concomitantly. The whole process lasts ∼90 min. Black holes correspond to CB nuclei. For all figures of the manuscript, dorsal (ectoderm side) is up and ventral (amnioserosa side) is down. Bars, 4 µm.

circulatory system (Rizki, 1978; Rugendorff et al., 1994). The *D. melanogaster* cardiac tube is made of two rows of 52 myoendothelial cells (cardioblasts [CBs]) enclosing a lumen. The cardiac myoendothelium originates from migrating mesodermal cells, which undergo a mesenchymal–epithelial transition to form two bilateral rows of cells attached to each other by adherens junctions (Rugendorff et al., 1994; Tepass and Hartenstein, 1994; Fremion et al., 1999). During dorsal closure, the two rows of CBs, together with adjacent pericardial cells, migrate as a sheet of cells in association and coordination with the overlying ectoderm (Chartier et al., 2002). They eventually meet each other at the dorsal midline, make new adherens junctions, and start forming a lumen that enlarges during the late stages of embryogenesis (Rugendorff et al., 1994; Haag et al., 1999).

The genetic control of the *D. melanogaster* cardiac tube morphogenesis has been extensively studied (Zaffran and Frasch, 2002; Monier et al., 2007; Tao and Schulz, 2007). These studies have provided a better understanding on how affecting gene function can perturb general organ morphogenesis, cell number, and cell identity. However, only few studies have characterized, at a cellular level, the consequences of gene inactivation on cardiac cell morphogenesis.

In this study, formation of the *D. melanogaster* cardiac tube lumen was revisited by providing a detailed analysis of cardiac cell morphogenesis. Using in vivo 3D and time-lapse imaging and analyzing the distribution of various molecular markers led to the definition of distinct membrane domains to which specific functions in lumen formation can be attributed. To evaluate the functional importance of cell shape changes, membrane specification, and remodeling, we searched for mutations affecting these aspects of cardiac cell morphogenesis. We have identified *slit*, *roundabout* (*robo*), *dystroglycan* (*dg*), and *held out wings* (*how*) as key components of a genetic pathway that controls cardiac cell morphogenesis and is required for correct lumen formation. Moreover, our data provide evidence for a mechanism of tube formation substantially distinct from the so-far described mechanisms of epithelial tubulogenesis.

Results

CB morphogenesis during cardiac tube formation

We have restricted our analysis to the CBs, as the cardiac tube lumen is exclusively formed by the membrane walls of these cells. To investigate CB morphogenesis during formation of the cardiac tube, the expression of Dmoesin-GFP (Fig. 1), which binds to cortical actin (Polesello et al., 2002), or directly to actin-GFP (see Fig. 2, A–L), was targeted to CBs using the 24B-Gal4

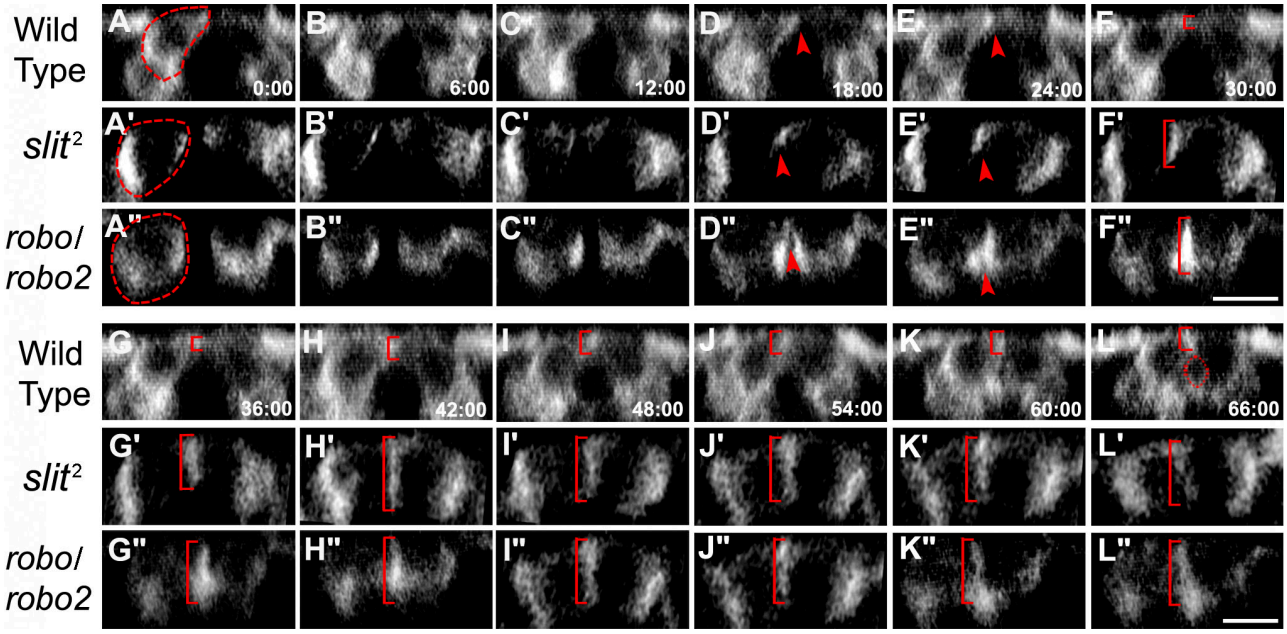

Figure 2. **Slit–Robo functions are required to form the cardiac lumen.** Reconstructed time-lapse Z views (6-min intervals) taken from videos (Videos 2–4, available at http://www.jcb.org/cgi/content/full/jcb.200801100/DC1) illustrating CB shape changes and lumen formation in wild-type (24B-Gal4; UAS actin-GFP; A–L), *slit*^{2} mutant (A′–L′), and *robo/robo2* double mutant embryos (A″–L″) from stages 14–16 of embryogenesis. Mutant alleles are in 24B-Gal4; UAS actin-GFP background to visualize CB shape. Wild-type CBs change their shape from rounded (not depicted), to pearlike (A), to crescentlike (L), whereas the CBs of both mutants (*slit*^{2} or *robo/robo2*) remain rounded over the entire period (from A′–L′ to A″–L″). (A, A′, and A″) Red dotted lines delimit the CB shape. Note the highly dynamic actin-GFP accumulation at the sites of cell–cell contact. CBs contact first by the "leading edge" domains (D–D″ and E–E″) where accumulation of actin-GFP (arrowheads) is observed. This cell–cell contact is dramatically enlarged in *slit*^{2} and *robo/robo2* mutants (F–F″ and L–L″, brackets). (L) Red dotted line labels the newly formed lumen, absent in *slit*^{2} (L′) and *robo/robo2* (L″) mutants. Bars, 5 µm.

driver and the binary Gal4–upstream activating sequence (UAS) system. Time-lapse confocal imaging was used to record GFP and to follow actin dynamics during the coalescence of the two bilateral rows of CBs (Videos 1 and 2, available at http://www.jcb.org/cgi/content/full/jcb.200801100/DC1). To focus this analysis on the membrane domains that are directly implicated in lumen formation, transverse Z sections were generated from the reconstructed 3D views at different developmental time points. This allowed us to efficiently follow CB shape changes at different steps of cardiac tube formation (Fig. 1).

At the onset of dorsal closure, CBs adopt a pearlike shape consecutive to constriction of their domain facing the dorsal midline (Fig. 1, F and F', compared with Fig. 1, E and E'). Actin-rich cytoplasmic extensions grow from this membrane domain, which constitutes the leading edge of the dorsally migrating CBs (Fig. 1 B, arrowheads). CBs from each of the two rows come progressively into contact at their leading edges and join at the dorsal midline (Fig. 1, B, G, and G'). Subsequently, CBs adopt a crescentlike shape (Fig. 1, H and H'), which allows their bases to join ventrally and thus to close the tube (Fig. 1, I and I'), creating an internal lumen. During this step, which takes ∼60 min (see Fig. 2 and Videos 1 and 2), the dorsal part of CBs detaches from the dorsal ectoderm. Throughout this process, CBs increase their size and keep growing after tube closure; as a result, the lumen enlarges progressively (Fig. 1, D and I). Thus, our in vivo analysis provides for the first time a step by step description of the dynamics of cardiac tube formation. It confirms previous observations (Rugendorff et al., 1994; Haag et al., 1999) made on fixed preparations and provides, in addition, a highly tractable new method for analyzing in vivo CB cell behavior in wild-type and mutant backgrounds.

Slit–Robo signaling is required for CB cell shape changes during lumen formation

To investigate the genetic control of cell behavior during cardiac tubulogenesis, we tested several candidate genes known to be expressed in migrating CBs and in the cardiac tube. We first analyzed the function of *slit*, encoding an extracellular protein that binds to the membrane receptors Robo and acts either as attractant or repellent (Dickson and Gilestro, 2006). Slit is expressed in CBs (Rothberg et al., 1988) and, recently, three studies have reported that Slit–Robo pathway function is required for normal assembly of the cardiac tube, CB migration, and lumen formation (Qian et al., 2005; MacMullin and Jacobs, 2006; Santiago-Martinez et al., 2006). Loss of *slit* function leads to composite phenotypes, such as misaligned or twisted tube portions, gaps in one row of CBs, and, at some places, when the two opposite CB rows have coalesced, lack of lumen or formation of an abnormal lumen. Thus, Slit–Robo signaling plays a key role during the late steps of cardiac development, but none of the previous studies have addressed precisely how cell morphogenesis is affected when the Slit–Robo pathway is inactivated.

To better understand this issue, we used CB-targeted live imaging of actin-GFP. Changes in the CB cell shapes were recorded in wild type, *slit*^{2}, or *robo/robo2* double mutant embryos (Fig. 2 and Videos 2–4, available at http://www.jcb.org/cgi/content/full/jcb.200801100/DC1). We found, in contrast to the wild type, that the mutant CBs (in both *slit* and *robo/robo2* mutant

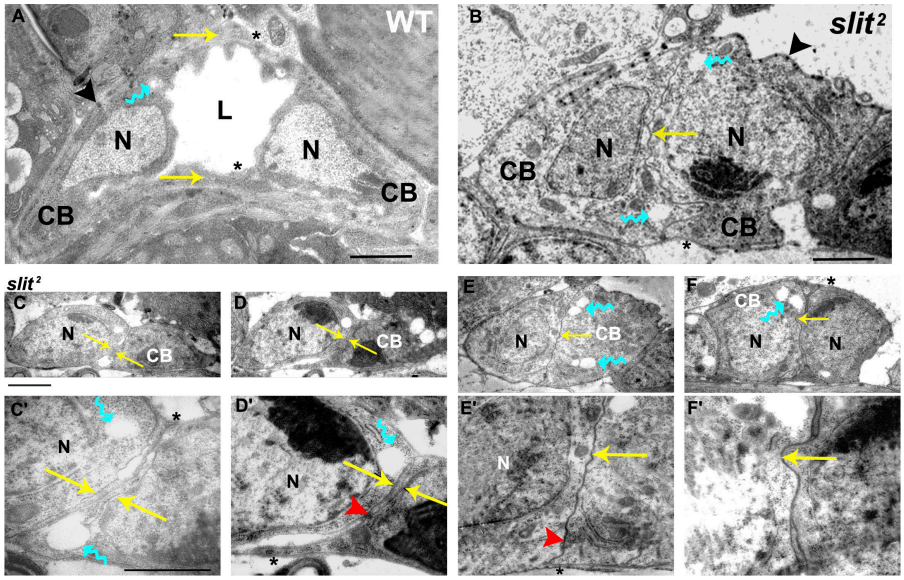

Figure 3. **Ultrastructure of *slit*^{2} mutant CBs.** (A–F) Transverse ultra-thin sections of wild-type (A) and *slit*^{2} mutant embryos (B–F) at late stage 17. (C–F) Ultra-thin sections at different levels along the AP axis, with C the most anterior and F the most posterior. (C′–F′) High magnifications of C–F showing the extending cell–cell contact between the CBs of the opposite rows (yellow arrows), compared with the wild type (A). (B–F) In *slit*^{2} mutant embryos, CBs have a much more rounded shape than in wild-type embryos (A) and the lumen is not formed. (C′ and D′) Note that in *slit*^{2} mutants, the contact between CBs often shows interruptions where some vacuolelike structures are observed (blue arrows). L, lumen; CB, cardioblast; N, nucleus; yellow arrows, cell–cell contact; black arrowheads, hemi-adherens junctions; red arrowheads, adherens junction; asterisks, basement membrane. Bars, 1 µm.

backgrounds) do not modulate their shape during migration (Fig. 2, A' and A", compare with Fig. 2 A). Mutant CBs keep their initial round shape (Fig. 2, A'–C' and A"–C"), do not constrict to form a dorsal leading edge with filopodia, and do not detach from the overlying dorsal ectoderm. As a consequence, CBs come into contact with the opposite row by their entire nonconstricted dorsal membrane surfaces, forming a large dorsal cell–cell contact extending ventrally (Fig. 2, F'–L' and F"–L" [bracket], compared with Fig. 2, F–L). Thus, when the two rows of mutant CBs succeed in joining at the dorsal midline, the presumptive lumen domain is either absent or displaced ventrally, preventing its normal juxtaposition with the contralateral luminal surface and blocking lumen formation (Fig. 2, L' and L", compared with Fig. 2 L).

The in vivo observations have been confirmed by an electron microscopy analysis of wild-type and *slit*^{2} mutant cardiac tubes showing the lack of cell shape changes in *slit*^{2} mutant CBs, which, in contrast to wild-type CBs, display a round shape (Fig. 3, compare B with A). The progressive shrinking of the CB cytoplasm at the site of initial cell–cell contact, which contributes to the lumen formation in wild type, is strongly affected (Fig. 3 A and Fig. S1 [available at http://www.jcb.org/cgi/content/full/jcb.200801100/DC1], yellow arrows, compared with Fig. 3 B). Cell–cell contacts between the two opposite CBs spread over a much larger area than in the wild-type situation. This extended area of cell–cell contact in *slit*^{2} mutant embryos is most probably caused by the lack of cell shape remodeling in the absence of *slit* function. Electron-dense dots corresponding to adherens junctions between two CBs are detected in *slit*^{2} mutants (Fig. 3, D' and E') in the same position as in the wild type (Fig. S1 B), indicating that *slit* mutants are able to differentiate cell junctions. This general phenotype is recovered along the entire anterior–posterior axis, at least in the region where the two rows of cells have coalesced (Fig. 3, C–F). However, slight variation in this general phenotype is observed consisting essentially of interruptions in the firm cell–cell contacts between CBs that sometimes form vacuolelike structures inside the CB cytoplasm (Fig. 3, B–F, blue arrows). Similar structures are also observed at early stages in wild-type embryos (Fig. S1 A, blue arrows).

Characterization of distinct CB membrane domains directly involved in lumen formation

To better understand the cellular mechanisms regulating cardiac lumen formation, we analyzed the distribution of cell polarity markers in developing wild-type CBs. CB precursors originate from nonpolarized mesenchymal cells of the dorsal mesoderm. After germ band retraction, they form two bilateral rows of polarized cells sharing some polarity features with epithelial cells (Fremion et al., 1999). CBs possess a basal domain adjacent to the overlying ectoderm, expressing classical markers of basement membranes; extracellular matrix proteins, including laminin A (Yarnitzky and Volk, 1995), perlecan (Terribly reduced optic lobes [Trol] in *D. melanogaster*; Fig. 4 B; Voigt et al., 2002), pericardin (a type IV collagenlike protein; Chartier et al., 2002), Slit (Fig. 4 C; Rothberg et al., 1988), and their receptors, Dg (Fig. 4 A); integrins; and Robo (Stark et al., 1997; Qian et al., 2005). CBs also contain basal-lateral domains expressing Discs large (Dlg; Fig. S2, A and C, available at http://www.jcb.org/cgi/content/full/jcb.200801100/DC1), α-spectrin, and adherens junction markers such as β-catenin (Armadillo [Arm] in *D. melanogaster*), and DE-Cadherin (DE-Cad; or Shotgun [Shg] in *D. melanogaster*; Fremion et al., 1999; Haag et al., 1999), from which adherens junctions among cells of the same CB rows are formed (Fig. 4 D', arrowheads).

In the following, we refer to luminal domains (L domains) and adherent domains (J domains) to designate the membrane domains involved in the formation of the lumen walls and adherens junctions responsible for the dorsal and ventral sealing of the tube, respectively.

CBs were assumed to display "apical-basal" polarity, based on the absence of α-spectrin expression in the domain facing the dorsal midline (Fremion et al., 1999). However, this membrane domain never shows any expression of the known classical apical

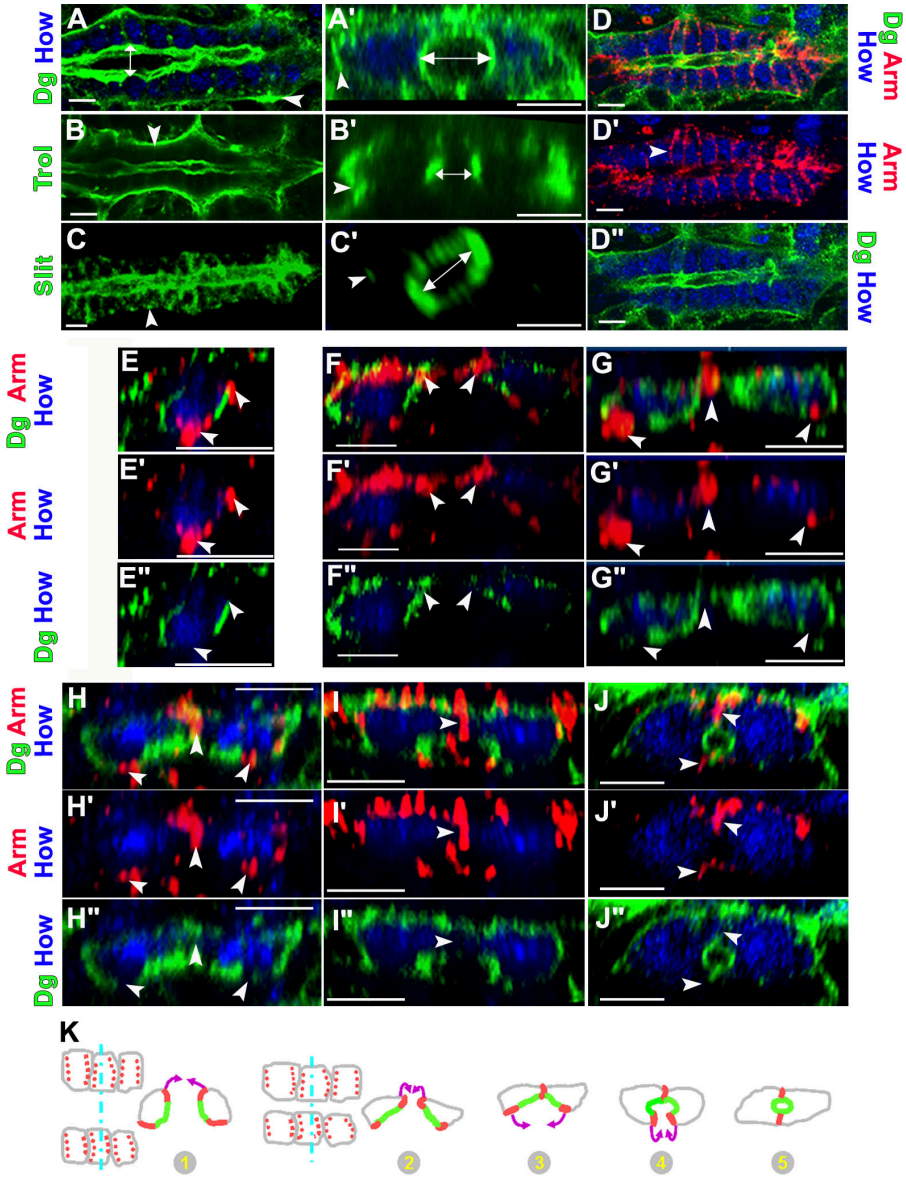

Figure 4. **Characterization of distinct CB membrane domains involved in lumen formation.** Dorsal XY views of wild-type cardiac tubes (A–C and D–D'') and reconstructed Z views of wild-type CBs (A'–C', E–J, E'–J', and E''–J''). (A and A') Dg (green) and How (blue, showing CB nuclei) staining. (B and B') Trol expression revealed using Trol-GFP reporter. (C and C') Slit expression. Notice that Dg, Trol, and Slit are expressed at the basal side (arrowheads) and at the luminal side (double-sided arrows) of the CBs in the membrane domain forming the lumen (L domain). (D–D'') Wild-type embryo stained with antibodies against Arm (red), Dg (green), and How (blue) at stage 16. (D', arrowhead) Arm is localized in the basolateral membranes involved in cell–cell contact between CBs of the same row. (E–J) Merged Z views of wild-type CBs from stages 13–14 in E to stage 16 in J, stained with antibodies against Arm (red), Dg (green), and How (blue). (E'–J' and E''–J'') The same views as E–J showing Arm and How (E'–J') or Dg and How staining (E''–J''). Arm is localized at the future contact between the two CBs (arrowheads), at the dorsal leading edge, and at the ventral side. Arm is excluded from Dg-positive domain (basal and luminal faces), before (E–E'', arrowheads), during (F–I, F'–I', and F''–I'', arrowheads), and after CB migration (J–J'', arrowheads). When CBs join dorsally, Arm is strongly expressed at the site of contact between the two CBs (G–J, G'–J', and G''–J'', arrowheads). When the ventral sides join to close the tube, Arm is specifically localized at the site of cell–cell contacts (dorsal and ventral; J and J', arrowheads) and excluded from the lumen domain where Dg is expressed (J''). The Arm-positive domains and forming adherens junctions between CBs of opposite rows are called J domains. (K) Schematic representation of CB morphogenesis during cardiac tube formation. Gray, CBs; red, Arm; green, Dg; blue dashed lines, Z section positions; purple arrows, CB shape changes. (1) Before CB migration, CBs are rather round and already express Arm in the J domains and Dg in the L domains. (2) CBs constrict and form a leading edge dorsally. (3) They join first dorsally, then adopt a crescentlike shape (4), and finally meet ventrally and close the tube (5). Bars, 4 μm.

markers of epithelial cells, including Crumbs (Tepass et al., 1990; Qian et al., 2005), β-heavy-spectrin, Bazooka, or atypical PKC (unpublished data), indicating that CBs cannot be considered as classical apical-basal polarized epithelial cells. The apical-like spectrin-free domain of CBs corresponds to the F-actin–rich leading edge or J domain that extends filopodia and contacts dorsally with the CBs of the opposite row.

In contrast, the future lumen membrane domain expresses classical basal components such as Slit (Fig. 4, C and C'), Dg (Fig. 4, A and A'; Qian et al., 2005), integrins (not depicted), and Trol (Fig. 4, B and B'). This membrane domain, the L domain, constitutes the wall of the lumen and actively contributes to the deposition of an extracellular matrix within the growing lumen (Fig. S1, asterisks; Rugendorff et al., 1994; Chartier et al., 2002).

We complemented this analysis of CB polarity by examining the localization of Arm as a marker for potential cell–cell junctions. Arm starts to localize at the future J domains (dorsally, at the leading edge, and ventrally; Fig. 4, E–J and E'–J', arrowheads) significantly before the joining of the two CB rows at the dorsal midline. In the course of CB row migration, Arm becomes excluded from the future L domains, where Dg (Fig. 4, E''–J''), Trol, and Slit are localized (not depicted). This specific localization of Arm is maintained during CB migration and after fusion of the bilateral cardiac primordia (Fig. 4, F–J and F'–J') and marks the sites of the adherens junctions, seen by electronic microscopy (Fig. S1 B''), which are responsible for tube sealing. In a similar manner, another adherens junction marker, DE-Cad, is also observed at the J domains of CBs (not depicted), as well as classical basolateral markers, Dlg (Fig. S2, B and D) and Lethal giant larvae (Lgl; not depicted).

Altogether these observations define distinct membrane domains involved in lumen formation: the L domain expressing Dg, Slit, and Trol in which cell–cell adhesion is prevented,

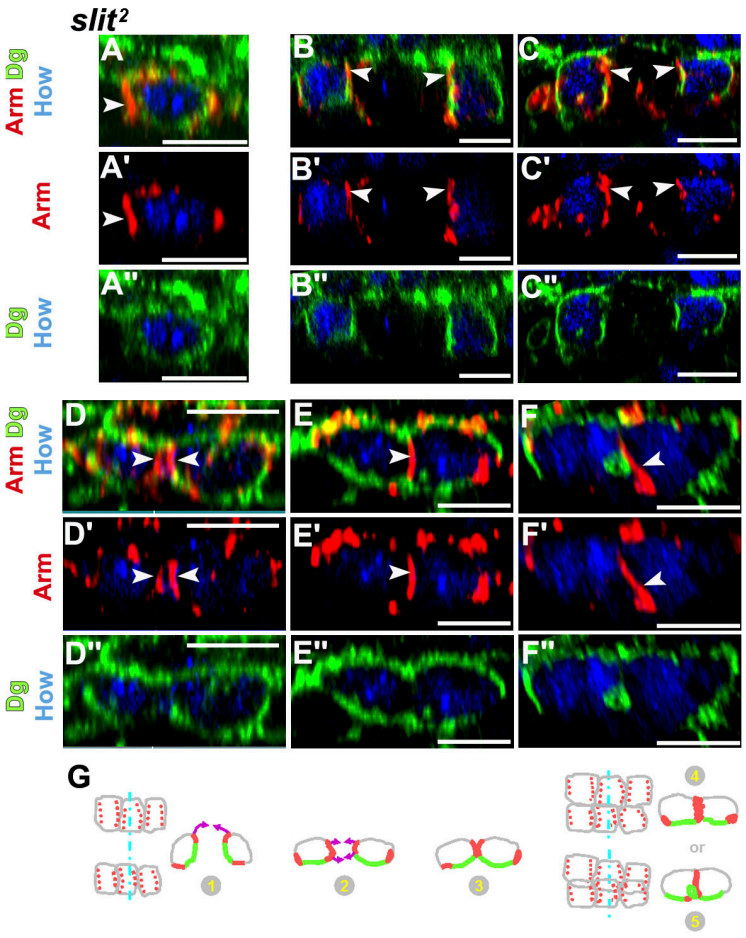

Figure 5. **Aberrant setting of CB membrane domains in *slit*^{2} mutant embryos.** (A–F) Merged Z views of CBs from *slit*^{2} mutant embryos stained with Arm (red), Dg (green), and How (blue) antibodies at different stages of embryogenesis (from stages 13–14 in A to stage 16 in F). A′–F′ show Arm and How, whereas A″–F″ show Dg and How staining. CBs keep their initial rounded shape during all stages of cardiac tube formation. Initially, Arm is correctly localized at the future J domains (arrowheads), but is not completely excluded from the Dg-positive domain as it is in the wild type (A′–C′, compared with Fig. 4, E′ and F′). When CBs join dorsally, Arm shows an extended area of expression compared with the wild type (Fig. 5, E and E′ [arrowheads], compare with Fig. 4, G–H and G′–H′). Finally, in a few cases a lumen can be detected, Arm is localized all along the extended dorsal J domain (Fig. 5 F, compare arrowheads with Fig. 4 J). (G) Schematic representation of CB shape dynamics and membrane domains in *slit*^{2} mutant embryos (compare with Fig. 4 K). Step 1 is similar to that of the wild type except that the Arm-positive domain is larger in the mutant, and, as a consequence, Dg and Arm partially colocalize. (2) In the mutant, CBs do not change their shape, do not form a leading edge (3), and make contact by an enlarged Arm-positive J domain. Finally, CBs are either not able to form a lumen (4) or, rarely (5), they show an ectopic small lumen formed ventrally. Bars, 4 µm.

surrounded by two J domains where Arm is localized and responsible for sealing the tube dorsally and ventrally (Fig. 4 K). *D. melanogaster* CBs appear to show specific cell polarity with prepatterned L domains with basal membrane properties. In contrast to so-far described models of tubulogenesis, the cardiac lumen is formed from a basallike and not from an apical membrane domain.

The Slit–Robo pathway is involved in the specification and the differentiation of the lumen-forming membrane domain

As CB cell shape changes do not occur in *slit*^{2} mutant embryos (Figs. 2 and 3), we decided to investigate the involvement of the Slit–Robo pathway in specifying CB membrane domains by analyzing Arm and Dg expressions in *slit*^{2} mutant embryos (Fig. 5). As in wild-type embryos, Arm is observed in the J domains (Fig. 5, A′–F′), as well as Dlg (Fig. S2, B and D) and Lgl (not depicted). However, from the onset of CB migration onward, the Arm-positive domain is clearly expanded and maintained, or even increased when CBs come into contact (Fig. 5, E′ and F′). Correlatively, Arm is first found to partially colocalize with Dg (Fig. 5, A–C). During CB migration, Dg is progressively excluded from the Arm-positive domain to become completely absent from this domain (Fig. 5, D–F) in the cases when the two contralateral CBs make contact (mean of 60% of the CBs constituting the mutant cardiac tube can reach this stage), Dg is displaced toward the ventral boundary of the Arm J domain, underlining, in some cases, an ectopic, small lumenlike structure (Fig. 5 F). Interestingly, Dg is also sometimes recovered at the periphery of these lumenlike structures located inside the cytoplasm of the CB cells (Fig. S3 A, arrows, available at http://www.jcb.org/cgi/content/full/jcb.200801100/DC1). Together, these observations suggest that Slit–Robo function is required for setting the nonadherent L domain, which is critical for the formation of a correct lumen (Fig. 5 G).

How and Dg also contribute to the setting of the lumen-forming membrane domain

The aforementioned results indicate that the establishment of specialized CB membrane domains is a crucial step for cardiac lumen formation. To gain further insights into this process, we searched for other genes whose activity could be required for setting CB membrane domains. Previous studies demonstrated that *dg* and *how* are involved in late aspects of cardiac development or function (Zaffran et al., 1997; Qian et al., 2005; unpublished data), and thus we decided to test their role in CB morphogenesis.

How encodes an RNA-binding protein of the Star family implicated in mRNA translation control and gene splicing (Nabel-Rosen et al., 2002; Volohonsky et al., 2007). The formation of the cardiac lumen has been investigated in the hypomorphic

how18 mutants (Zaffran et al., 1997), in which no How expression in the cardiac tube can be detected (Fig. S4, available at http://www.jcb.org/cgi/content/full/jcb.200801100/DC1). Electron microscopy analysis in *how18* mutant CBs (Fig. 6) shows the lack of cell shape changes and the extension of cell–cell contacts (Fig. 6, B and C, yellow arrows). These mutant CBs form nonswollen lumenlike gaps filled with extracellular matrix material (Fig. 6 C, asterisk) that intrude into the CB cytoplasm and are highly convoluted (Fig. 6 compared with Fig. S1).

The misspecification of the lumen membrane domain in *how* mutants is supported by the reduced and displaced ventral staining of the L domain marker Dg (Fig. 7 F, compare with Fig. 4 J). As a consequence, the Arm-positive domain is now extended along almost the entire region of cell–cell contacts between CBs of the opposite rows (Fig. 7, A–F). A partial colocalization of Arm and Dg is observed, principally during the migration step (Fig. 7, A' and B', compared with Fig. 7, A" and B"). Importantly, as in *slit*^{2} mutants, the CB shape and membrane domains remodeling observed in the wild type does not occur (Fig. 7, E and F). CBs do not constrict their leading edge at the onset of migration and remain rounded, with large Arm-positive J domains facing the dorsal midline (Fig. 7, C and D).

In a similar way we tested lumen formation in *dg* mutants. Dg is an extracellular matrix receptor and is a part of the widely expressed and evolutionary conserved Dystrophin complex (Winder, 2001). In *D. melanogaster*, Dg has been shown to be required for epithelial organization, polarity, and muscle viability (Deng et al., 2003; Schneider et al., 2006; Shcherbata et al., 2007).

As in *dg* deficiency Df(2R)JP6Dg (Qian et al., 2005), earlier cardiac defects make the analysis of lumen formation difficult, so we opted to use partial loss-of-function *dg* alleles, *dg62*, *dg323*, and *dg248* (Deng et al., 2003; Schneider et al., 2006; Shcherbata et al., 2007). They give rise to essentially the same type of phenotypes, so we present only data for the *dg62* allele. We observed that most of the homozygous *dg* mutants (80%, first group) form a tube with a general wild-type appearance; however, the L domains remain stacked, with no or a very small lumen formed (Fig. 7, G–L). A small proportion (5%, second group) of *dg* mutant embryos shows a strong phenotype in cardiac tube morphogenesis: migration defects, gaps in the cardiac rows, and twisted tubes similar to phenotypes recovered in *slit*^{2} mutant and in *dg* Df(2R)JP6Dg deficiency (Fig. S2, E and F; Qian et al., 2005). The last 15% of *dg* mutants display a wild-type phenotype. Precise localization of cell polarity markers has therefore been investigated only in the first group of mutant embryos. All along the anterior–posterior axis, the L domain, revealed by Trol, is considerably reduced compared with wild type, at the expense of the J domain, probed by Arm expression (Fig. 7, G–L). Moreover, as in *how18* and *slit*^{2} mutants, the dynamics of cell shape remodeling observed in wild-type embryos does not occur (Fig. 7, G–L); the CBs remain rounded with no constriction of the dorsal J domain. A partial colocalization of Arm and Trol is also observed during the CBs migration step (Fig. 7, G'–L' and G"–L").

Because *slit*, *dg*, and *how* mutants share common phenotypes, we analyzed Slit localization in *how18* and *dg62* mutant

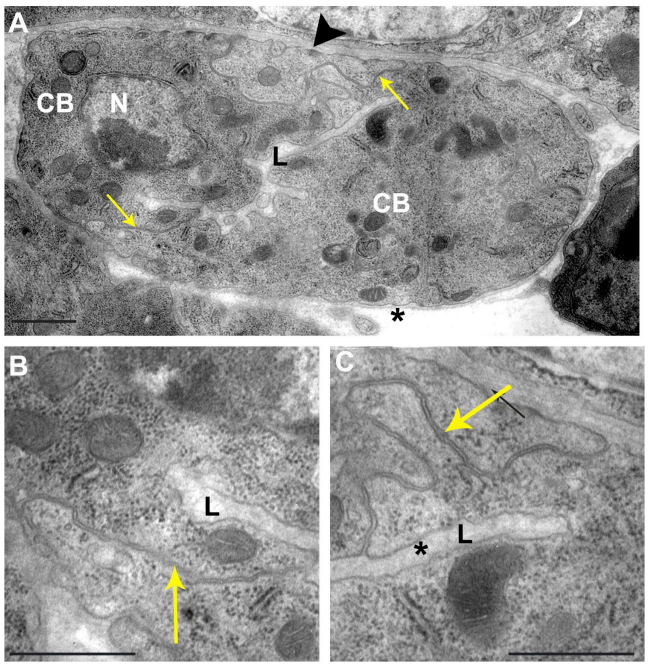

Figure 6. **Ultrastructure of *how18* mutant CBs.** (A–C) Ultra-thin sections of *how18* mutant embryo at late stage 17. (B and C) High magnifications of A showing the J domains at both sides of the embryo (yellow arrows). Note that CBs are very round compared with the wild type (compare A with Fig. 3 A) but L domains are conserved. However, the lumen does not swell and shows numerous circumvolutions. Abbreviations and annotations are the same as in Fig. 3. Bars, 1 µm.

embryos (Fig. 8). At the end of CB migration (Fig. 8, I, J, and N, compared with Fig. 8 D) and when the tube is closed (Fig. 8, K–M and O–R, compared with Fig. 8, E–H), Slit expression is no longer recovered at the L domain or into the cytoplasm just underneath the L domain, but is found to predominantly localize randomly in the cytoplasm in both mutants. Occasionally, Slit expression is still present within the small and generally ectopic lumen (Fig. S3 B). Slit is also found in association with Dg or Trol in cytoplasmic vacuolelike structures, also observed in *slit*^{2} mutants (Fig. S3 A).

To investigate genetic epistasis between *slit*, *how*, and *dg*, we first analyzed the effects of Slit overexpression in the cardiac tubes of *how18* and *dg62* homozygous mutant embryos. Remarkably, both Slit localization at the L domain and lumen formation (in 60% of *how18* mutants) are rescued by Slit overexpression in the CBs of *how18* homozygous mutants (Fig. 9). In contrast, Slit overexpression is not able to rescue lumen formation in *dg62* cardiac tubes (not depicted). These results suggest that *how* acts upstream of *slit* and that *dg* functions parallel to *slit* to control lumen formation.

In addition, we observed that *slit* genetically interacts with *how* and *dg* for the formation of the cardiac lumen. A mutant phenotype in lumen formation is observed in 80% of *slit*^{2}/*how18* transheterozygotes (Fig. 5 A) and in 73% of *slit*^{2}/*dg62* transheterozygotes (Fig. 5 B), which is never observed in single heterozygotes. Finally, overexpression of Dg in CBs leads to a similar phenotype as *dg* loss of function, showing a strong ectopic Slit localization in the cytoplasm and a very

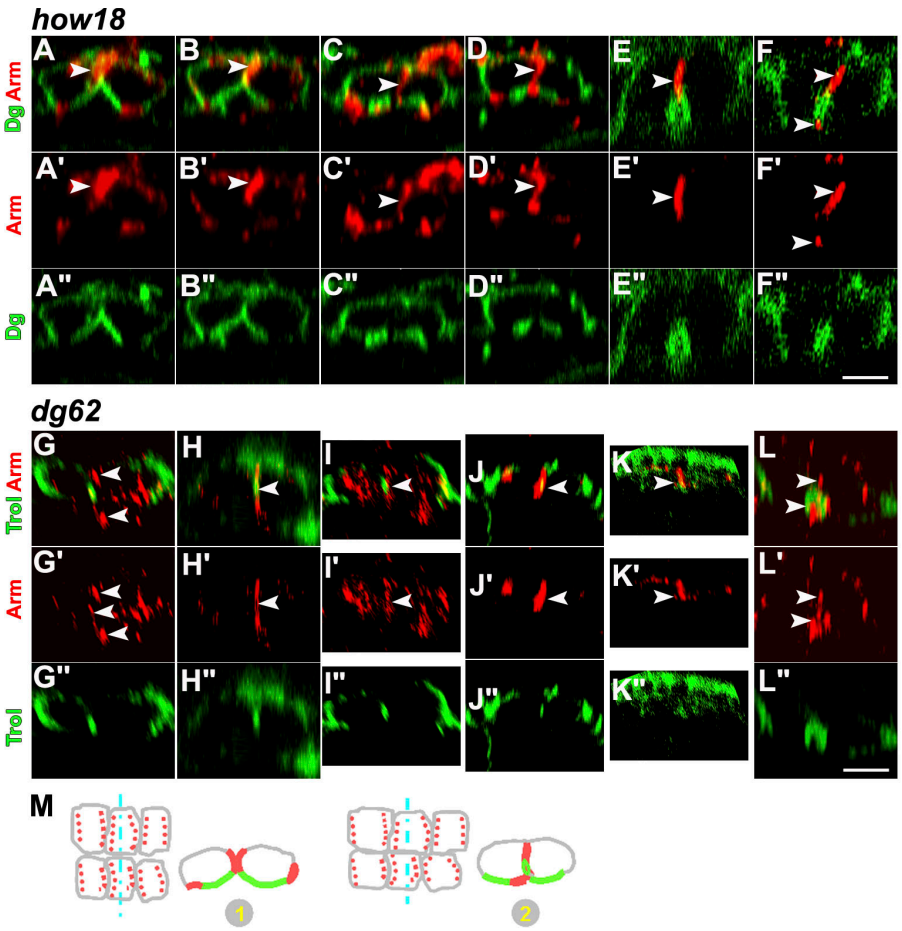

Figure 7. **Abnormal CB membrane domains in *how18* and *dg62* mutant embryos.** (A–F) Transverse Z views of CBs from *how18* mutant embryos at different stages of development (from stages 14–16) stained for Arm (red) and Dg (green). (A′–F′ and A″–F″) The same views showing staining for Arm or Dg only. Arm expression is spread toward the ventral side of the CBs, colocalizing partially with Dg (A′, B′, A″, and B″). Notice that CBs do not change their shape or constrict; they behave similarly to what is observed in *slit*^{2} mutant embryos. (G–L) Transverse Z views of CBs from *dg62* mutant embryos stained for Arm (red) and for Trol (*D. melanogaster* perlecan, green). (G′–L′ and G″–L″) The same views as G–L, showing Arm or Trol staining only. *dg* mutant CBs do not change their shape (G″–L″) and resemble *how* mutant CBs. The dorsal J domain enlarged compared with the wild type (H′ and J′–L′ [arrowheads], compared with Fig. 4 G′) and overlaps with the Trol-positive L domains. (M) Diagram summarizing the observations in *how18* and *dg62* mutant embryos. Compare the extension and localization of J and L domains with wild-type embryos (Fig. 4 K). Arrowheads show the dorsal J domain expressing Arm. Bars, 4 µm.

narrow lumen (Fig. S5, C and D, available at http://www.jcb.org/cgi/content/full/jcb.200801100/DC1).

Altogether, these observations support that *slit*, *how*, and *dg* participate in the same pathway to control cardiac lumen formation.

Discussion

A mechanism of lumen formation distinct from that proposed for epithelial tubulogenesis

The analysis provided here, using both in vivo cell imaging and subcellular localization of molecular markers, establishes the cellular basis of lumen formation of the *D. melanogaster* cardiac tube. As previously reported, the lumen of the tube is formed from the migration of two bilateral rows of polarized CBs, which join at the dorsal midline (Rugendorff et al., 1994; Fremion et al., 1999; Haag et al., 1999). One main result of our study is the characterization of two types of cell membrane domains directly involved in lumen formation, the J domains and the L domain. Adherens junctions that are responsible for sealing the tube originate from the J domain, whereas the membrane walls of the lumen originate from the L domain.

Remarkably, the L domain displays characteristics of basal membranes, revealed by expression of molecular markers normally associated with a basal membrane. Furthermore, specification of the L and J domains takes place very early in the tubulogenesis process, significantly before coalescence of the bilateral rows of CBs at the dorsal midline. Finally, during CB migration, membrane domains undergo remodeling, concomitant with profound cell shape changes. These two cellular processes appear to be closely connected and are probably regulated by the cellular environment of the CBs composed by the overlying dorsal ectoderm and the amnioserosa cells. These interactions will be investigated in a future work.

The mechanism of *D. melanogaster* cardiac lumen formation reported here (Fig. 10 A) is thus notably different from the previously described mechanisms of epithelial tubulogenesis (Myat, 2005). In epithelial tubulogenesis, after receiving a polarization signal that sets apicobasal polarity, the cells or group of cells establish a basal surface and generate vesicles carrying apical membrane proteins. The vesicles are targeted to the prospective apical region, where they fuse with the existing membrane or with each other to form a lumen (Kamei et al., 2006; Kerman et al., 2006). Finally, continued vesicle fusion and apical secretion expand the lumen.

In contrast, constriction of the leading edge domain during CB migration, precise control of cell shape changes, and delimitation of specific membrane domains appear to be the driving forces of *D. melanogaster* cardiac lumen formation. Cells forming the dorsal vessel have the features of migrating cells. In contrast

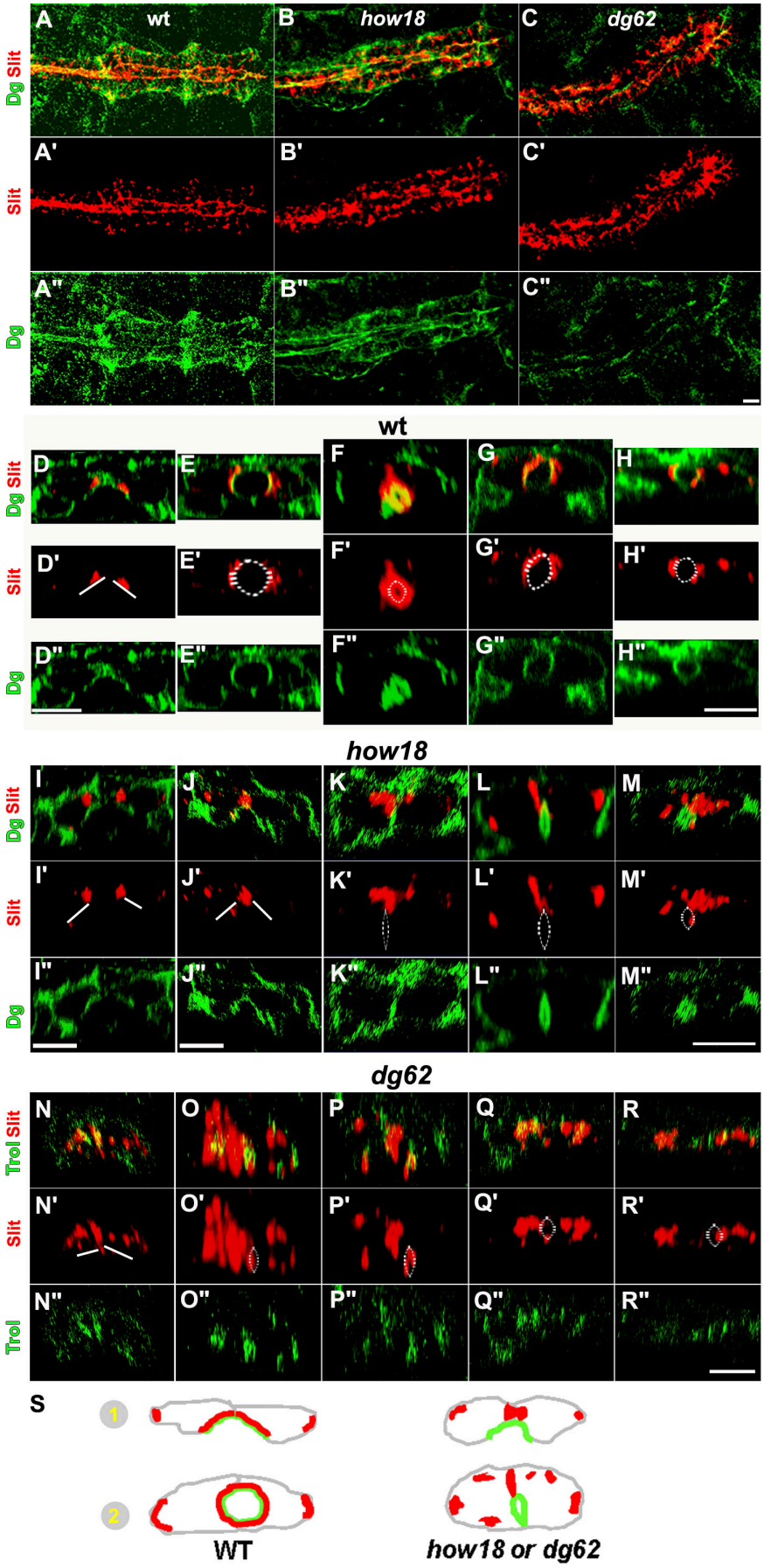

Figure 8. **Slit is mislocalized in *how18* and *dg62* mutant CBs.** (A–C) Dorsal XY views of wild-type (A), *how18* (B), and *dg62* (C) embryos at stage 16 showing general distribution of Dg and Slit within the cardiac tube. (D–R) Transverse Z views of CBs from wild-type (D–H), *how18* (I–M), and *dg62* (N–R) embryos at stage 16 stained for Slit and Dg (D–M) and for Slit and Trol (N–R). A′–R′, Slit only; A″–M″, Dg only; N″–R″, Trol only. Slit is strongly expressed at the L domains colocalizing with Dg (A and D–H) during (D) and at the end (E–H) of CB migration . In *how18* (B) and *dg62* (C), Slit is no longer observed at the L domains and does not colocalize with Dg or Trol, but is rather seen inside the cytoplasm in dense patches during CB migration (e.g., compare D–D″ with I–I″) and after (K–R, K′–R′, and K″–R″, compared with E–H, E′–H′, and E″–H″). Solid and dotted lines show the expected wild-type localization of the L domain. (S) Schematic representation of Slit expression (red) and Dg or Trol (green). During migration (1) and after CB coalescence (2), Slit is expressed in patches inside CB cytoplasm in *how* or *dg* mutant instead of being expressed at the L domains as in wild type. Bars, 5 μm.

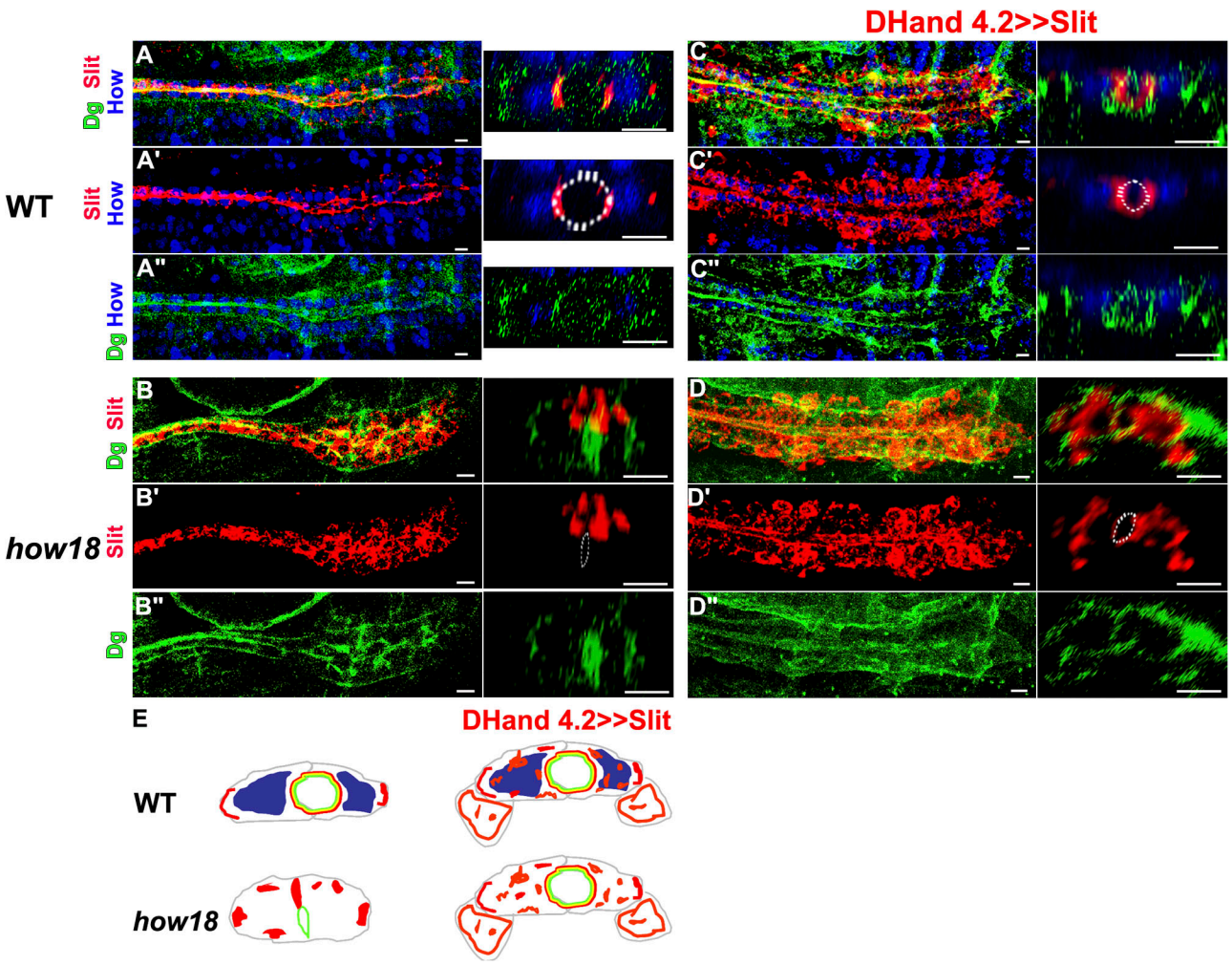

Figure 9. **Slit expression in CBs rescues Slit localization and lumen formation in *how18* mutants.** (A–D) Cardiac tubes of stage 16 embryos stained with Dg (green), Slit (red), and How (blue). A′–D′, Slit only; A″–D″, Dg only. (A–D) On the left are dorsal XY views of wild-type (A and C) and *how18* mutant (B and D) embryos; and on the right, transverse Z views of the same cardiac tube. (C and D) Slit overexpression under the control of Hand-Gal4, showing a random distribution of Slit in the cytoplasm of the CBs and of the pericardial cells. Slit is also recovered at the L domain of the CBs. (C) In a wild-type background, Slit overexpression does not affect cardiac lumen formation. Although *how18* mutant CBs (B) show a strongly reduced lumen and an absence of Slit at the L domain (Fig. 8, I–M), Slit overexpression in this *how18* mutant CBs (D) restores lumen formation and Slit localization at the L domain (in addition to its strong expression in the cytoplasm and pericardial cells because of its overexpression). Dashed circles delimit the lumen. (E) A cartoon showing Slit localization and the cardiac lumen in the different conditions depicted in A–D: wild-type (A), *how18* mutant (B), Slit overexpression in a wild-type background (C), and Slit overexpression in a *how18* mutant background (D). Bars: (all panels except B) 5 µm; (B) 4 µm.

to epithelial tubulogenesis, which involves apical membrane domains, the apex of polarized CBs constricts, forms adherens junctions, and consequently does not constitute the L domain. Instead, the luminal membrane domain possesses basal membrane characteristics, as is also the case in endothelial cells (Davis and Senger, 2005). Moreover, the size of the cardiac lumen is determined by the isotropic growth of CBs, and not, as in other models, by anisotropic extension of the L domain involving apical membrane vesicles. Finally, the genetic control of the process involves gene products of *slit*, *robo*, *how*, and *dg*, which are not known regulators of lumen formation in epithelial tubes.

Function of *slit*, *robo*, *how*, and *dg* in cardiac lumen formation

Our study leads to the identification of a genetic pathway, including *slit*, *robo*, *how*, and *dg*, controlling membrane domain specification and dynamics during cardiac lumen formation. Within this pathway, Slit appears to play a central role and a previously unrecognized function in cell morphogenesis.

Several studies have shown that Slit–Robo function is essential for cardiac tube formation by controlling the proper migration, cohesion, and alignment of the two rows of CBs (Qian et al., 2005; MacMullin and Jacobs, 2006; Santiago-Martinez et al., 2006). The results reported here show that Slit is also involved in the correct specification of the L domain and its distinct features with respect to the adjacent J domains. Activation of Slit–Robo signaling determines the respective size of these two types of domains.

Our data suggest that activation of this pathway inhibits the formation of adherens junctions. This possibility is supported by recent findings in chick retina cells, where activation of the Slit–Robo pathway leads to the inactivation of β-catenin

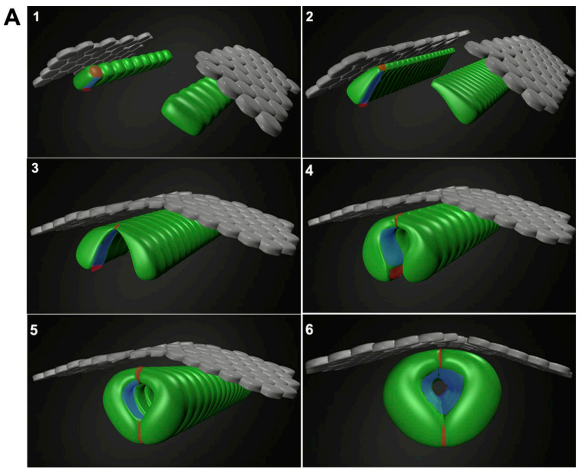

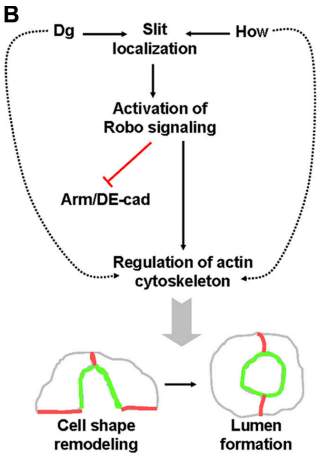

Figure 10. **Model of action of Slit, How, and Dg during cardiac tube formation.** (A) Diagram of 3D views of CBs (green) with the ectoderm (gray). Arm/DE-Cad–positive domains are visualized in red, and Dg, Slit–Robo, and Trol-positive domains in blue. (1–6) The key steps of cell behavior leading to cardiac lumen formation are represented. (B) Schematic representation of the interactions between Slit, Robo, How, and Dg in CBs to control specification and differentiation of the J and L membrane domains and to participate in lumen formation and growth. Dotted arrows, hypothetic interactions; black arrows, activation; red line, inhibition; gray, CBs; red, J domains; green, L domains.

(Arm in *D. melanogaster*), resulting in the dissociation of N-cadherin from the junctional complex and preventing the formation of adherens junctions (Rhee et al., 2002, 2007). Consistent with these observations, DE-Cad (Shg) is expressed in the J domains of CBs (unpublished data) and is required for cardiac tube morphogenesis (Haag et al., 1999). Moreover, *slit* and *shg* show genetic interaction in cardiac tube morphogenesis (Qian et al., 2005). In the absence of *slit* function, the size of the L domain is strongly reduced (Fig. 5, A–C), suggesting that Slit–Robo signaling prevents the formation of Arm/DE-Cad–mediated adherens junctions in the L domain.

How encodes an RNA-binding protein involved in mRNA metabolism, and given its exclusive nuclear localization at this stage of development (Fig. S4), How may regulate *slit* splicing. In the absence of the How protein, the gene splicing could be affected, producing a Slit protein unable to correctly localize at the L domain. This hypothesis is consistent with the fact that expression of wild-type Slit in CBs can suppress the effect of *how18* mutation on Slit localization and lumen formation. How has also recently been shown to regulate the splicing of neuronal membrane proteins such as neurexin (Edenfeld et al., 2006). Moreover, How is expressed in the midline glia with Slit and Dg (Fig. S4 C), suggesting that interaction among these three genes is part of a general mechanism by which junctions and lumen formation are controlled.

A model for the genetic control of lumen formation in the cardiac tube, based on our observations, is proposed in Fig. 10 B. According to this model, How could directly regulate Slit by controlling its splicing and targeting the luminal compartment. Consequently, Slit binds to Robo activating the signaling pathway, which in turn inhibits Arm/DE-Cad–mediated adherens junction formation in the luminal compartment, leading then to the specification of distinct J and L domains. Parallel to this, activation of Slit–Robo signaling modulates the actin cytoskeleton and triggers CB cell shape remodeling required for lumen formation and growth. As How is able to act on many targets, it could also directly control the actin cytoskeleton by targeting an actin-binding molecule. Concerning Dg, we have shown that *dg* and *slit* genetically interact (Fig. S5 B); however, overexpression of Slit does not rescue the lumen phenotype observed in *dg* mutants, contrasting with *how* mutations. Thus, we propose that Dg could regulate Slit localization at the L domain by its function in the specification and differentiation of the L domain, and therefore acts parallel to *slit* for lumen formation, behaving, for example, as a coreceptor of Robo. In addition, Dg could control actin cytoskeleton dynamics via its interaction with Dystrophin.

A model of endothelial tubulogenesis applicable to axial vessel and heart tube formation in vertebrates?

Our data clearly show that cardiac tube formation in *D. melanogaster* differs substantially from all other described mechanisms of tubulogenesis. Is this mechanism of tubulogenesis unique or is it shared with other organs and/or other organisms? Primary vasculogenesis in vertebrates leads to the formation of large median vessels, the dorsal aorta and the cardinal vein (Pardanaud et al., 1987; Torres-Vazquez et al., 2003; Jin et al., 2005). These vessels arise from migrating mesenchymal cells of the lateral mesoderm, termed angioblasts, that are organized in bilateral groups of cells. Angioblasts migrate toward the midline as a cohort of cells, coalesce, and form a lumen. At this stage, as in flies, cells around the lumen show a crescentlike shape (Risau, 1995; Jin et al., 2005) and an extracellular matrix is deposited at the internal face of luminal membranes (Davis and Senger, 2005). Similar cellular events are also observed during the formation of the primitive cardiac tube in vertebrates (Harvey, 2002), suggesting that a common mechanism of tubulogenesis might exist for all tubes that arise from the coalescence of migrating bilateral mesenchymal cells.

As proposed by Hartenstein and Mandal (2006), the *D. melanogaster* cardiac tube, or dorsal vessel, shares many similarities with the cardiovascular system of vertebrates. A significant fraction of genes expressed in the *D. melanogaster* cardiac tube are also annotated to be expressed in vertebrate blood vessels, suggesting that vasculogenesis and dorsal vessel morphogenesis might share common genetic regulators.

Finally, components of the genetic pathway controlling cardiac lumen formation that we describe here have potentially similar functions in vertebrates. It has been shown previously that numerous proteins involved in axon guidance are expressed in vertebrate blood vessels (for review see Weinstein, 2005). In particular, the Slit–Robo signaling pathway has been involved

in promoting tumor vascularization, hSlit2 being expressed in tumor cells and hRobo1 in endothelial cells (Wang et al., 2003). Moreover, mSlit3 has been implicated in mammalian cardiogenesis (Liu et al., 2003), and Quaking, the mouse homologue of How, is required for vasculogenesis and expressed in the developing heart (Noveroske et al., 2002).

In conclusion, our analysis of CB morphogenesis during development of the *D. melanogaster* cardiovascular system provides evidence for a new model of biological tube formation. We propose that this mechanism might also be used for the formation of the large median vessels and primitive heart tube in vertebrates.

Materials and methods

D. melanogaster strains

For live experiments, we used a UAS Dmoesin-GFP; 24B-Gal4 line and UAS actin-GFP; 24B-Gal4 line to follow cardiac cell behaviors. The UAS Dmoesin-GFP was obtained from F. Payre (Centre de Biologie du Développement, Toulouse, France; Polesello et al., 2002) and the UAS-actin GFP was obtained from the Kyoto Stock Center. The flies *slit*^{2}; UAS-actin GFP and *robo*^{GA285}, *robo2*^{4}; UAS actin-GFP were crossed with the *slit*^{2} or *robo*^{GA285}, *robo2*^{4} mutant flies carrying 24B-GAL4 driver. Wild-type flies are Oregon lines. Trol-GFP line has been obtained from the L. Cooley laboratory (L. Cooley, Yale University Medical School, New Haven, CT; Kelso et al., 2004). As mutant flies, we used *slit*^{2}/CyOWg-LacZ, (Bloomington Stock Center), double mutant *robo*^{GA285}, *robo2*^{4}/CyOWg-LacZ and *robo*^{GA285}, *robo2*^{8}/CyOWg-LacZ (provided by B. Dickson, Institute für Mechanik, Vienna, Austria; Rajagopalan et al., 2000), *how18*/TM3actGFP (Zaffran et al., 1997), *dg62*/CyOWg-lac-Z, *dg248*/CyOWg-lac-Z, and *dg323*/CyOGFP (provided by S. Baumgartner, Lund University, Lund, Sweden; Deng et al., 2003). Mutants were selected by the absence of βGal/GFP staining. To overexpress Dg we used 24B-Gal4 and UAS-Dg full length obtained from M. Schneider (Lund University; Schneider et al., 2006). To overexpress Slit, we used 24B-Gal4 and Hand-Gal4 (DHandGal4 4.2) from A. Paululat (Osnabrück University, Osnabrück, Germany) as drivers and UAS Slit from B. Dickson.

Antibodies

For the primary antibodies, we used rabbit anti-Dg, 1:300 (provided by W.M. Deng, Florida State University, Tallahassee, Florida; Deng et al., 2003); rabbit anti-Trol, 1:1,000 (Schneider et al., 2006); rabbit anti-β3-tubulin, 1:1,000 (Developmental Studies Hybridoma Bank [DSHB]); mouse anti-Arm, 1:100 (DSHB); mouse anti-Dlg, 1:100 (DSHB); mouse anti-Slit, 1:50 (DSHB; amplification with Renaissance TSA Biotin system [PerkinElmer]); rabbit anti-Lgl, 1:500 (provided by J. Knoblich, Institute für Mechanik; Betschinger et al., 2003); rat anti-How, 1:100 (provided by T. Volk, Weissman Institute, Rehovot, Israel; Nabel-Rosen et al., 1999); mouse anti-Prc, 1/3 (Chartier et al., 2002); mouse anti-βGal, 1:500 (Promega); and mouse and rabbit anti-GFP, 1/500 (Invitrogen).

For secondary antibodies, we used Biotin SP conjugated anti–mouse (Jackson ImmunoResearch Laboratories), 1:500, and Cy5 anti–rat and anti–rabbit, 1:100 (Jackson ImmunoResearch Laboratories); Alexa 546 anti–mouse and anti–rabbit, 1:500; and Alexa 488 anti–mouse and anti–rabbit, 1:500 (Invitrogen).

Immunostaining

Embryos were collected from 12 to 16 h, dechorionated in bleach for 5 min, fixed in PBS/heptane (1:1), 4% formaldehyde, for 20 min, and devitellinized in heptane/methanol (1:1), washed in methanol and ethanol, and rehydrated progressively in PBS. Embryos were blocked in PBS, 0.1% Tween, and 10% BSA and incubated overnight at 4°C with the primary antibody. Embryos were washed with PBS, 0.1% Tween, and 0.1% BSA and incubated for 1–2 h with the secondary antibody, washed again, and mounted in Fluoromount medium (SouthernBiotech).

Heat fixation for Arm staining

After dechorionation, embryos were fixed by heat fixation method: they were plunged for 5–7 s in a boiling solution with 68 mM NaCl and 0.04% Triton X-100. They were put for a few minutes on ice and prepared for devitellinization as described in the previous section.

Confocal analysis and time-lapse records

Embryos expressing UAS actin-GFP (or UAS Dmoesin-GFP) under the control of 24B-Gal4 driver in wild-type, *slit*^{2}, and *robo*^{GA285}, *robo2*^{4} mutant backgrounds were dechorionated in bleach (2 min), rinsed in water, placed on a coverslip in the appropriate orientation, and then mounted in 3 M of oil (Voltalef) for live imaging using a confocal microscope. Images compiled from 0.5-µm optical sections were collected every 6 min. All the preparations were visualized on confocal microscopes (LSM 510 or 510 Meta; Carl Zeiss, Inc.) at room temperature using a plan Apochromat 20× 0.8 NA or a C Apochromat (water) 40× 1.2 NA lens (Carl Zeiss, Inc.). 4D reconstructions and image analysis were performed using LSM browser, Zen 2007 light edition (Carl Zeiss, Inc.), Volocity 4.0 (Improvision), Imaris 4.0 (Bitplane), and Photoshop CS2 (Adobe) softwares.

Electron microscopy

Embryos were dechorionated in bleach for 3 min. They were transferred into a microfuge tube on ice and fixed for ∼20 h with 2% glutaraldehyde and 2% paraformaldehyde in 0.1 M cacodylate buffer, pH 7.4. They were washed several times in cacodylate buffer and postfixed for 2 h on ice in 1% osmium tetroxide and 2% glutaraldehyde in 50 mM cacodylate buffer. After dehydratation the specimens were embedded in epon 812. Ultra-thin sections (80 nm) were done on a UCT ultramicrotome (Leica). They were analyzed with an electron microscope (912; Carl Zeiss, Inc.) and the images were taken with a camera (Bioscan 792; GATAN) using digital micrograph software.

Model building

The model of cardiac tube morphogenesis (Fig. 10 A) has been built using Blender 4.22.

Online supplemental material

Video 1 depicts the CB morphogenesis in the course of cardiac lumen formation and is the basis for building Fig. 1. Videos 2–4 allow the building of Fig. 2. Video 2 shows actin dynamics during cardiac lumen formation, and Videos 3 and 4 reveal the requirement of *slit* and *robo/robo2* functions, respectively, in cardiac lumen formation.

Fig. S1 presents the ultrastructure of wild-type CBs at different stages of cardiac tube development. Dlg localization in wild-type and *slit*^{2}, *dg62*, and *how18* mutants is described in Fig. S2. Additional examples of cardiac tube phenotypes in *slit*^{2}, *dg62*, *how18*, and *dg323* mutant embryos are observed in Fig. S3. Fig. S4 describes How expression in the cardiac tube and in the midline glia. Finally, transheterozygous mutant embryos, *slit*^{2}/*how18* or *slit*^{2}/*dg62*, have been analyzed for their cardiac lumen defects in Fig. S5. Online supplemental material is available at http://www.jcb.org/cgi/content/full/jcb.200801100/DC1.

We thank S. Baumgartner, W.M. Deng, J. Knoblich, and M. Schneider for antibodies and all the helpful material and advice they provided. We are grateful to T. Volk and to the Developmental Studies Hybridoma Bank for antibodies; B. Dickson, A. Paululat, the Bloomington Stock Center, and the Kyoto Stock Center for fly stocks; and to J. Gros for his help in building the model of cardiac tube formation using Blender. We also thank R. Kelly, T. Lecuit, and S. Zaffran for advice and helpful discussions; M. Gettings for critical reading of the manuscript; J.P. Chauvin, A. Aouane, and J.P. Arsanto for electron microscopy studies; P. Weber for imaging; and S. Long and F. Graziani for fly assistance.

This work was supported by the Centre National de la Recherche Scientifique, the Institut Nationale de la Santé et de la Recherche Médicale, the Association de la Recherche contre le Cancer, and the Association Française contre les Myopathies. C. Medioni was supported by a postdoctoral fellowship from the Association de la Recherche contre le Cancer and M. Zmojdzian by a postdoctoral Institut Nationale de la Santé et de la Recherche Médicale fellowship.

Submitted: 16 January 2008
Accepted: 23 June 2008

References

Betschinger, J., K. Mechtler, and J.A. Knoblich. 2003. The Par complex directs asymmetric cell division by phosphorylating the cytoskeletal protein Lgl. *Nature.* 422:326–330.

Chartier, A., S. Zaffran, M. Astier, M. Semeriva, and D. Gratecos. 2002. Pericardin, a *Drosophila* type IV collagen-like protein is involved in the morphogenesis and maintenance of the heart epithelium during dorsal ectoderm closure. *Development.* 129:3241–3253.

Davis, G.E., and D.R. Senger. 2005. Endothelial extracellular matrix: biosynthesis, remodeling, and functions during vascular morphogenesis and neovessel stabilization. *Circ. Res.* 97:1093–1107.

Deng, W.M., M. Schneider, R. Frock, C. Castillejo-Lopez, E.A. Gaman, S. Baumgartner, and H. Ruohola-Baker. 2003. Dystroglycan is required for polarizing the epithelial cells and the oocyte in *Drosophila*. *Development.* 130:173–184.

Dickson, B.J., and G.F. Gilestro. 2006. Regulation of commissural axon pathfinding by slit and its Robo receptors. *Annu. Rev. Cell Dev. Biol.* 22:651–675.

Edenfeld, G., G. Volohonsky, K. Krukkert, E. Naffin, U. Lammel, A. Grimm, D. Engelen, A. Reuveny, T. Volk, and C. Klambt. 2006. The splicing factor crooked neck associates with the RNA-binding protein HOW to control glial cell maturation in *Drosophila*. *Neuron.* 52:969–980.

Fremion, F., M. Astier, S. Zaffran, A. Guillen, V. Homburger, and M. Sémériva. 1999. The heterotrimeric protein G_o is required for the formation of heart epithelium in *Drosophila*. *J. Cell Biol.* 145:1063–1076.

Haag, T.A., N.P. Haag, A.C. Lekven, and V. Hartenstein. 1999. The role of cell adhesion molecules in *Drosophila* heart morphogenesis: faint sausage, shotgun/DE-cadherin, and laminin A are required for discrete stages in heart development. *Dev. Biol.* 208:56–69.

Hartenstein, V., and L. Mandal. 2006. The blood/vascular system in a phylogenetic perspective. *Bioessays.* 28:1203–1210.

Harvey, R.P. 2002. Patterning the vertebrate heart. *Nat. Rev. Genet.* 3:544–556.

Jin, S.W., D. Beis, T. Mitchell, J.N. Chen, and D.Y. Stainier. 2005. Cellular and molecular analyses of vascular tube and lumen formation in zebrafish. *Development.* 132:5199–5209.

Kamei, M., W.B. Saunders, K.J. Bayless, L. Dye, G.E. Davis, and B.M. Weinstein. 2006. Endothelial tubes assemble from intracellular vacuoles in vivo. *Nature.* 442:453–456.

Kelso, R.J., M. Buszczak, A.T. Quinones, C. Castiblanco, S. Mazzalupo, and L. Cooley. 2004. Flytrap, a database documenting a GFP protein-trap insertion screen in *Drosophila melanogaster*. *Nucleic Acids Res.* 32:D418–D420.

Kerman, B.E., A.M. Cheshire, and D.J. Andrew. 2006. From fate to function: the *Drosophila* trachea and salivary gland as models for tubulogenesis. *Differentiation.* 74:326–348.

Liu, J., L. Zhang, D. Wang, H. Shen, M. Jiang, P. Mei, P.S. Hayden, J.R. Sedor, and H. Hu. 2003. Congenital diaphragmatic hernia, kidney agenesis and cardiac defects associated with Slit3-deficiency in mice. *Mech. Dev.* 120:1059–1070.

Lubarsky, B., and M.A. Krasnow. 2003. Tube morphogenesis: making and shaping biological tubes. *Cell.* 112:19–28.

MacMullin, A., and J.R. Jacobs. 2006. Slit coordinates cardiac morphogenesis in *Drosophila*. *Dev. Biol.* 293:154–164.

Monier, B., F. Tevy, L. Perrin, M. Capovilla, and M. Sémériva. 2007. Downstream of homeotic genes: in the heart of Hox function. *Fly.* 1:59–67.

Myat, M.M. 2005. Making tubes in the *Drosophila* embryo. *Dev. Dyn.* 232:617–632.

Nabel-Rosen, H., N. Dorevitch, A. Reuveny, and T. Volk. 1999. The balance between two isoforms of the *Drosophila* RNA-binding protein how controls tendon cell differentiation. *Mol. Cell.* 4:573–584.

Nabel-Rosen, H., G. Volohonsky, A. Reuveny, R. Zaidel-Bar, and T. Volk. 2002. Two isoforms of the *Drosophila* RNA binding protein, how, act in opposing directions to regulate tendon cell differentiation. *Dev. Cell.* 2:183–193.

Noveroske, J.K., L. Lai, V. Gaussin, J.L. Northrop, H. Nakamura, K.K. Hirschi, and M.J. Justice. 2002. Quaking is essential for blood vessel development. *Genesis.* 32:218–230.

Pardanaud, L., C. Altmann, P. Kitos, F. Dieterlen-Lievre, and C.A. Buck. 1987. Vasculogenesis in the early quail blastodisc as studied with a monoclonal antibody recognizing endothelial cells. *Development.* 100:339–349.

Polesello, C., I. Delon, P. Valenti, P. Ferrer, and F. Payre. 2002. Dmoesin controls actin-based cell shape and polarity during *Drosophila melanogaster* oogenesis. *Nat. Cell Biol.* 4:782–789.

Qian, L., J. Liu, and R. Bodmer. 2005. Slit and Robo control cardiac cell polarity and morphogenesis. *Curr. Biol.* 15:2271–2278.

Rajagopalan, S., E. Nicolas, V. Vivancos, J. Berger, and B.J. Dickson. 2000. Crossing the midline: roles and regulation of Robo receptors. *Neuron.* 28:767–777.

Rhee, J., N.S. Mahfooz, C. Arregui, J. Lilien, J. Balsamo, and M.F. VanBerkum. 2002. Activation of the repulsive receptor Roundabout inhibits N-cadherin-mediated cell adhesion. *Nat. Cell Biol.* 4:798–805.

Rhee, J., T. Buchan, L. Zukerberg, J. Lilien, and J. Balsamo. 2007. Cables links Robo-bound Abl kinase to N-cadherin-bound beta-catenin to mediate Slit-induced modulation of adhesion and transcription. *Nat. Cell Biol.* 9:883–892.

Risau, W. 1995. Differentiation of endothelium. *FASEB J.* 9:926–933.

Rizki, T.M. 1978. M. The Circulatory System and Associated Cell Tissues: The Genetics and Biology of *Drosophila.* Vol. 2b. M. Ashburner and T.R.F. Wright, editors. Academic Press, New York. 55 pp.

Rothberg, J.M., D.A. Hartley, Z. Walther, and S. Artavanis-Tsakonas. 1988. slit: an EGF-homologous locus of *D. melanogaster* involved in the development of the embryonic central nervous system. *Cell.* 55:1047–1059.

Rugendorff, A., A. Younossi-Hartenstein, and V. Hartenstein. 1994. Embryonic origin and differentiation of the *Drosophila* heart. *Dev. Genes Evol.* 203:266–280.

Santiago-Martinez, E., N.H. Soplop, and S.G. Kramer. 2006. Lateral positioning at the dorsal midline: Slit and Roundabout receptors guide *Drosophila* heart cell migration. *Proc. Natl. Acad. Sci. USA.* 103:12441–12446.

Schneider, M., A.A. Khalil, J. Poulton, C. Castillejo-Lopez, D. Egger-Adam, A. Wodarz, W.M. Deng, and S. Baumgartner. 2006. Perlecan and Dystroglycan act at the basal side of the *Drosophila* follicular epithelium to maintain epithelial organization. *Development.* 133:3805–3815.

Shcherbata, H.R., A.S. Yatsenko, L. Patterson, V.D. Sood, U. Nudel, D. Yaffe, D. Baker, and H. Ruohola-Baker. 2007. Dissecting muscle and neuronal disorders in a *Drosophila* model of muscular dystrophy. *EMBO J.* 26:481–493.

Stark, K.A., G.H. Yee, C.E. Roote, E.L. Williams, S. Zusman, and R.O. Hynes. 1997. A novel alpha integrin subunit associates with betaPS and functions in tissue morphogenesis and movement during *Drosophila* development. *Development.* 124:4583–4594.

Tao, Y., and R.A. Schulz. 2007. Heart development in *Drosophila*. *Semin. Cell Dev. Biol.* 18:3–15.

Tepass, U., and V. Hartenstein. 1994. The development of cellular junctions in the *Drosophila* embryo. *Dev. Biol.* 161:563–596.

Tepass, U., C. Theres, and E. Knust. 1990. crumbs encodes an EGF-like protein expressed on apical membranes of *Drosophila* epithelial cells and required for organization of epithelia. *Cell.* 61:787–799.

Torres-Vazquez, J., M. Kamei, and B.M. Weinstein. 2003. Molecular distinction between arteries and veins. *Cell Tissue Res.* 314:43–59.

Voigt, A., R. Pflanz, U. Schafer, and H. Jackle. 2002. Perlecan participates in proliferation activation of quiescent *Drosophila* neuroblasts. *Dev. Dyn.* 224:403–412.

Volohonsky, G., G. Edenfeld, C. Klambt, and T. Volk. 2007. Muscle-dependent maturation of tendon cells is induced by post-transcriptional regulation of stripeA. *Development.* 134:347–356.

Wang, B., Y. Xiao, B.B. Ding, N. Zhang, X. Yuan, L. Gui, K.X. Qian, S. Duan, Z. Chen, Y. Rao, and J.G. Geng. 2003. Induction of tumor angiogenesis by Slit-Robo signaling and inhibition of cancer growth by blocking Robo activity. *Cancer Cell.* 4:19–29.

Weinstein, B.M. 1999. What guides early embryonic blood vessel formation? *Dev. Dyn.* 215:2–11.

Weinstein, B.M. 2005. Vessels and nerves: marching to the same tune. *Cell.* 120:299–302.

Winder, S.J. 2001. The complexities of dystroglycan. *Trends Biochem. Sci.* 26:118–124.

Yarnitzky, T., and T. Volk. 1995. Laminin is required for heart, somatic muscles, and gut development in the *Drosophila* embryo. *Dev. Biol.* 169:609–618.

Zaffran, S., and M. Frasch. 2002. Early signals in cardiac development. *Circ. Res.* 91:457–469.

Zaffran, S., M. Astier, D. Gratecos, and M. Semeriva. 1997. The held out wings (how) *Drosophila* gene encodes a putative RNA-binding protein involved in the control of muscular and cardiac activity. *Development.* 124:2087–2098.